Hindawi
Mathematical Problems in Engineering
Volume 2021, Article ID 6644133, 12 pages
https://doi.org/10.1155/2021/6644133

Research Article

The Fractional Strain Influence on a Solid Sphere under Hyperbolic Two-Temperature Generalized Thermoelasticity Theory by Using Diagonalization Method

Hamdy M. Youssef,[1,2] **Alaa A. El-Bary**,[3] **and Eman A. N. Al-Lehaibi**[4]

[1]*Mathematics Department, Faculty of Education, Alexandria University, Alexandria, Egypt*
[2]*Mechanical Engineering Department, College of Engineering and Islamic Architecture, Umm Al-Qura University, Makkah, Saudi Arabia*
[3]*Basic and Applied Science Institute, Arab Academy for Science, Technology, and Maritime Transport, P. O. Box 1029, Alexandria, Egypt*
[4]*Mathematics Department, Al-Lith University College, Umm Al-Qura University, Al-Lith, Saudi Arabia*

Correspondence should be addressed to Hamdy M. Youssef; youssefanne2005@gmail.com

Received 23 October 2020; Revised 7 January 2021; Accepted 6 February 2021; Published 16 February 2021

Academic Editor: Nicholas Alexander

This article constructs a mathematical model based on fractional-order deformations for a one-dimensional, thermoelastic, homogenous, and isotropic solid sphere. In the context of the hyperbolic two-temperature generalized thermoelasticity theory, the governing equations have been established. Thermally and without deformation, the sphere's bounding surface is shocked. The singularities of the functions examined at the center of the world were decreased by using L'Hopital's rule. Numerical results with different parameter fractional-order values, the double temperature function, radial distance, and time have been graphically illustrated. The two-temperature parameter, radial distance, and time have significant effects on all the studied functions, and the fractional-order parameter influences only mechanical functions. In the hyperbolic two-temperature theory as well as in one-temperature theory (the Lord-Shulman model), thermal and mechanical waves spread at low speeds in the thermoelastic organization.

1. Introduction

The subject matter's primary concern is how to detect an exact model that simulates thermoelastic material's behavior. Researchers and authors have developed several models in which the waves in solids and thermoelastic materials have been transmitted. But not all these models succeed as one of the metrics of a good model is to give the experimental results with a finite speed of progress of mechanical and thermal waves. To talk about thermomechanical transition models with elastic materials, a wide area cannot be limited to study. Therefore, we will discuss some recent models that need to be addressed.

The thermoelasticity model has been developed by Chen and Gurtin, based on two different conductive and dynamic temperatures. The temperature differential is proportionate to the heat source [1]. In the two-temperature thermoelastic theory, Warren and Chen investigated wave propagation [2]. However, before Youssef updates this theory and creates a two-temperature generalized thermostat model, there will be no study of that theory [3]. In many applications and inquiries, Youssef and several other writers used this model [4–13]. Youssef and El-Bary have proven that the classical two-temperature generalized thermoelasticity model does not provide heat wave transmission at a finite speed [14]. Therefore, Youssef and El-Bary have changed this model and implemented a new two-temperature model based on different thermal conductivity rules, called hyperbolic two-temperature generalized thermoelasticity [14]. In that model, Youssef suggested that it is proportional to the heat

supply to differentiate between conductive temperature and dynamic temperature acceleration. The speed of thermal wave propagation is limited in this model. The two-temperature theory is considered as a type of generalization of the heat conduction equation. It helps us to separate the conductive thermal wave and dynamical thermal wave and study each wave and its effects on the materials.

The fact that fractional systems possess memory justifies this generalization, as the time evolution of romantic relationships is naturally impacted by memory [15, 16]. The fractional-order dynamic model could model various real materials more adequately than integer-order ones and provide a more adequate description of many actual dynamical processes [17, 18]. Thus, some new thermoelastic models based on the concept of fractional calculus were introduced. Magin and Royston developed the first model using the fractional deformation derivative characterizing the material's behavior [19]. A Hookean solid is the derivative's zero-order, while a Newtonian fluid is the one-order. The intermediate spectrum of the heat gives different orders of thermoviscoelastic substances [19].

Depending on the factional-order strain, Youssef launched another new theory of general thermoelasticity. The relationship between stress and strain is seen as a new and distinct addition to Duhamel-Neumann [20]. Youssef has solved thermoelasticity with fractional sequence strain in one dimension, half of the space of Biot, Lord-Shulman, Green-Lindsay, and Green-Naghdi type II [20]. Youssef solved many applications of thermoelasticity of infinite thermoelastic spherical medium [21–24]. Mukhopadhyay and Kumar studied the general thermoelastic interactions with the cavity in the unlimited medium [25]. Many authors solved problems of thermoelastic medium with spherical cavity [26–35].

Most of the authors who regarded their applications as the spherical medium faced the singularity problem in its center. Few authors, for example, Thibault and others, were able to solve this situation in the thermoelastic solid sphere using L'Hopital's rule to resolve this problem [36].

In the present investigation, a solid sphere in the context of hyperbolic two-temperature generalized thermoelasticity theory based on the fractional-order strain definition will be studied. The advantages of the current article are that it is considered more generalized model than the models that precede it and contains the results of a new theory with comparing it to the results of previous theories.

2. The Governing Equations

Consider a perfect, thermoelastic, conducting, and isotropic spherical body that occupies the region $\xi = \{(r, \psi, \phi) : 0 \le r \le a, 0 \le \psi \le 2\pi, 0 \le \phi < 2\pi\}$. We use a spherical coordinative system (r, ψ, ϕ) that displays the radial coordinate, colatitude, and longitude of a spherical system, without any forces on the body and initially calming where r is the sphere radius, as in Figure 1. When there is no latitude or longitudinal variance, the symmetry condition is fulfilled. Both state functions depend on the distance and time of the radius.

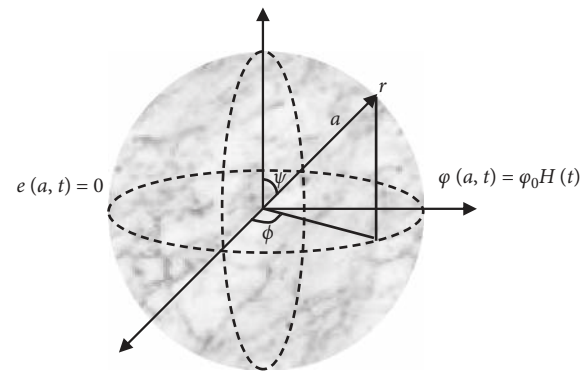

Figure 1: The isotropic homogeneous thermoelastic solid sphere.

We note that, due to spherical symmetry, the displacement components have the form

$$\left(u_r, u_\psi, u_\phi\right) = (u(r,t), 0, 0). \tag{1}$$

The equation of motion [10, 20] is

$$\rho\ddot{u} = (\lambda + 2\mu)\left(1 + \tau_1^\alpha D_t^\alpha\right)\frac{\partial e}{\partial r} - \gamma\frac{\partial T_D}{\partial r}. \tag{2}$$

The constitutive equations with damage mechanics variable [10, 20] are

$$\sigma_{rr} = \left(1 + \tau_1^\alpha D_t^\alpha\right)(2\mu e_{rr} + \lambda e) - \gamma\left(T_D - T_0\right), \tag{3}$$

$$\sigma_{\psi\psi} = \left(1 + \tau_1^\alpha D_t^\alpha\right)\left(2\mu e_{\psi\psi} + \lambda e\right) - \gamma\left(T_D - T_0\right), \tag{4}$$

$$\sigma_{\phi\phi} = \left(1 + \tau_1^\alpha D_t^\alpha\right)\left(2\mu e_{\phi\phi} + \lambda e\right) - \gamma\left(T_D - T_0\right), \tag{5}$$

$$\sigma_{r\phi} = \sigma_{\phi\psi} = \sigma_{r\psi} = 0. \tag{6}$$

The strain components are

$$\begin{aligned} e_{rr} &= \frac{\partial u}{\partial r}, \\ e_{\psi\psi} &= e_{\phi\phi} = \frac{u}{r}, \\ e_{r\phi} &= e_{\phi\psi} = e_{r\psi} = 0, \end{aligned} \tag{7}$$

where e is the cubical dilatation and it is given by

$$e = e_{rr} + 2e_{\phi\phi} = \frac{\partial u}{\partial r} + \frac{2u}{r} = \frac{1}{r^2}\frac{\partial\left(r^2 u\right)}{\partial r}. \tag{8}$$

The hyperbolic two-temperature heat conduction equations take the forms [10, 14, 20]

$$K\nabla^2 T_C = \rho C_E\left(\frac{\partial}{\partial t} + \tau_0\frac{\partial^2}{\partial t^2}\right)T_D + \gamma T_0\left(1 + \tau_1^\alpha D_t^\alpha\right)\left(\frac{\partial}{\partial t} + \tau_0\frac{\partial^2}{\partial t^2}\right)e, \tag{9}$$

$$\ddot{T}_D = \ddot{T}_C - c^2\nabla^2 T_C, \tag{10}$$

where $c\,(m/s)$ is the hyperbolic two-temperature parameter [14] and $\nabla^2 = (1/r^2)(\partial/\partial r)(r^2(\partial/\partial r))$.

The Riemann–Liouville fractional integral $I^{\alpha} f(t)$ description is used in the above equations written in a convolution type form [20, 37]

$$I^{\alpha} f(t) = \frac{1}{\Gamma(\alpha)} \int_0^t (t-v)^{\alpha-1} f(v)\mathrm{d}v, \quad t>0,\ \alpha>0, \tag{11}$$

which provides Caputo with the form of fractional derivatives:

$$D_t^{\alpha} f(t) = I^{-\alpha} f(t) = \begin{Bmatrix} \dfrac{1}{\Gamma(1-\alpha)} \displaystyle\int_0^t \frac{f(\xi)}{(t-\xi)^{\alpha}}\mathrm{d}\xi, & 0<\alpha<1, \\ f(t), & \alpha=0, \\ f'(t), & \alpha=1. \end{Bmatrix} \tag{12}$$

We consider that $\varphi = (T_C - T_0)$ and $\theta = (T_D - T_0)$ are the conductive and dynamical temperature increments, respectively. Then equations (2)–(5), (9), and (10) take the forms

$$\rho\ddot{u} = (\lambda+2\mu)\left(1+\tau_1^{\alpha}D_t^{\alpha}\right)\frac{\partial e}{\partial r} - \gamma\frac{\partial\theta}{\partial r}, \tag{13}$$

$$\sigma_{rr} = \left(1+\tau_1^{\alpha}D_t^{\alpha}\right)(2\mu e_{rr} + \lambda e) - \gamma\theta, \tag{14}$$

$$\sigma_{\psi\psi} = \left(1+\tau_1^{\alpha}D_t^{\alpha}\right)\left(2\mu e_{\psi\psi} + \lambda e\right) - \gamma\theta, \tag{15}$$

$$\sigma_{\phi\phi} = \left(1+\tau_1^{\alpha}D_t^{\alpha}\right)\left(2\mu e_{\phi\phi} + \lambda e\right) - \gamma\theta. \tag{16}$$

Equation (13) can be rewritten to be in the form

$$\rho\ddot{e} = (\lambda+2\mu)\left(1+\tau_1^{\alpha}D_t^{\alpha}\right)\nabla^2 e - \gamma\nabla^2\theta. \tag{17}$$

The following nondimensional variables are used for convenience [5, 9, 10]:

$$\begin{aligned} \{r', u', a'\} &= c_o\eta\{r, u, a\}, \\ \{t', \tau', \tau_o', \tau_1'\} &= c_o^2\eta\{t, \tau, \tau_o, \tau_1\}, \\ \{\theta', \varphi'\} &= \frac{1}{T_0}\{\theta, \varphi\}, \\ \sigma' &= \frac{\sigma}{\mu}. \end{aligned} \tag{18}$$

Then, we obtain

$$\ddot{e} = \left(1+\tau_1^{\alpha}D_t^{\alpha}\right)\nabla^2 e - b\nabla^2\theta, \tag{19}$$

$$\nabla^2\varphi = \left(\frac{\partial}{\partial t} + \tau_o\frac{\partial^2}{\partial t^2}\right)\theta + \varepsilon\left(\frac{\partial}{\partial t} + \tau_o\frac{\partial^2}{\partial t^2}\right)e, \tag{20}$$

$$\ddot{\theta} = \ddot{\varphi} - \tilde{c}^2\nabla^2\varphi, \tag{21}$$

$$\sigma_{rr} = \left(1+\tau_1^{\alpha}D_t^{\alpha}\right)\left(\beta^2 e - 2\frac{u}{r}\right) - \varepsilon_1\theta, \tag{22}$$

$$\sigma_{\psi\psi} = \left(1+\tau_1^{\alpha}D_t^{\alpha}\right)\left(\beta^2 e - 2\frac{\partial u}{\partial r}\right) - \varepsilon_1\theta, \tag{23}$$

$$\sigma_{\phi\phi} = \left(1+\tau_1^{\alpha}D_t^{\alpha}\right)\left(\beta^2 e - 2\frac{\partial u}{\partial r}\right) - \varepsilon_1\theta, \tag{24}$$

where $\gamma = (3\lambda+2\mu)\alpha_T$, $c_o^2 = (\lambda+2\mu)/\rho$, $\eta = \rho C_E/K$, $\varepsilon = \gamma/\rho C_E$, $\varepsilon_1 = \gamma T_o/\mu$, $\beta = ((\lambda+2\mu)/\mu)^{1/2}$, $b = \varepsilon_1/\beta^2$, and $\tilde{c}^2 = c^2/c_o^2$.

The primes are suppressed for simplicity.

The operator $\nabla^2 = (1/r^2)(\partial/\partial r)(r^2(\partial/\partial r))$ is singular at $r=0$; however, if symmetry prevails, the singularity will be reduced by the following L'Hopital's rule [36]:

$$\begin{aligned} \nabla^2\{e,\theta,\varphi\} &= \lim_{r\longrightarrow 0}\left[\frac{1}{r^2}\frac{\partial}{\partial r}\left(r^2\frac{\partial\{e,\theta,\varphi\}}{\partial r}\right)\right] \\ &= \lim_{r\longrightarrow 0}\left[\frac{\partial^2\{e,\theta,\varphi\}}{\partial r^2} + \frac{2}{r}\frac{\partial\{e,\theta,\varphi\}}{\partial r}\right] \\ &= \frac{\partial^2\{e,\theta,\varphi\}}{\partial r^2} + 2\frac{\partial^2\{e,\theta,\varphi\}}{\partial r^2}. \end{aligned} \tag{25}$$

Then, we get

$$\nabla^2\{e,\theta,\varphi\} = 3\frac{\partial^2}{\partial r^2}\{e,\theta,\varphi\}, \tag{26}$$

satisfying the boundary condition

$$\frac{\partial}{\partial r}\{e,\theta,\varphi\}|_{r=0} = 0. \tag{27}$$

Hence, we have

$$\begin{aligned} \nabla^2 e(r,t) &= 3\frac{\partial^2 e(r,t)}{\partial r^2}, \\ \nabla^2\theta(r,t) &= 3\frac{\partial^2\theta(r,t)}{\partial r^2}, \\ \nabla^2\varphi(r,t) &= 3\frac{\partial^2\varphi(r,t)}{\partial r^2}. \end{aligned} \tag{28}$$

By applying the form in (26) in equations (19)–(21), we obtain

$$\begin{aligned} \ddot{e} &= 3\left(1+\tau_1^{\alpha}D_t^{\alpha}\right)\frac{\partial^2 e}{\partial r^2} - 3b\frac{\partial^2\theta}{\partial r^2}, \\ 3\frac{\partial^2\varphi}{\partial r^2} &= \left(\frac{\partial}{\partial t} + \tau_o\frac{\partial^2}{\partial t^2}\right)\theta + \varepsilon\left(\frac{\partial}{\partial t} + \tau_o\frac{\partial^2}{\partial t^2}\right)e, \\ \ddot{\theta} &= \ddot{\varphi} - 3\tilde{c}^2\frac{\partial^2\varphi}{\partial r^2}. \end{aligned} \tag{29}$$

We apply the Laplace transform defined as

$$\ell\{f(t)\} = \overline{f}(s) = \int_0^{\infty} f(t)e^{-st}\mathrm{d}t. \tag{30}$$

The Laplace transform of the fractional derivative is defined as [37]

$$\ell\{D_t^\alpha f(t)\} = s^\alpha \overline{f}(s) - D_t^\alpha I^{1-\alpha} f(0^+), \quad 0 < \alpha < 1. \tag{31}$$

The following initial conditions have been assumed:

$$D_t^\alpha I^{1-\alpha}\{\theta(r,0^+), \varphi(r,0^+), e(r,0^+)\} = 0, \quad 0 < \alpha < 1,$$
$$\frac{\partial\theta(r,t)}{\partial t}\Big|_{t=0} = \frac{\partial\varphi(r,t)}{\partial t}\Big|_{t=0} = \frac{\partial e(r,t)}{\partial t}\Big|_{t=0} = 0. \tag{32}$$

Thus, equations (19)–(24) have the forms

$$s^2\overline{e} = 3\left(1 + \tau_1^\alpha s^\alpha\right)\frac{\partial^2\overline{e}}{\partial r^2} - 3b\frac{\partial^2\overline{\theta}}{\partial r^2}, \tag{33}$$

$$3\frac{\partial^2\overline{\varphi}}{\partial r^2} = \left(s + \tau_o s^2\right)\overline{\theta} + \varepsilon\left(s + \tau_o s^2\right)\overline{e}, \tag{34}$$

$$\overline{\theta} = \overline{\varphi} - \delta^2\frac{\partial^2\overline{\varphi}}{\partial r^2}, \tag{35}$$

$$\overline{\sigma}_{rr} = \left(1 + \tau_1^\alpha s^\alpha\right)\left(\beta^2\overline{e} - 2\frac{\overline{u}}{r}\right) - \varepsilon_1\overline{\theta}, \tag{36}$$

$$\overline{\sigma}_{\psi\psi} = \left(1 + \tau_1^\alpha s^\alpha\right)\left(\beta^2\overline{e} - 2\frac{\partial\overline{u}}{\partial r}\right) - \varepsilon_1\overline{\theta}, \tag{37}$$

$$\overline{\sigma}_{\phi\phi} = \left(1 + \tau_1^\alpha s^\alpha\right)\left(\beta^2\overline{e} - 2\frac{\partial\overline{u}}{\partial r}\right) - \varepsilon_1\overline{\theta}, \tag{38}$$

$$\overline{e} = \frac{1}{r^2}\frac{\partial\left(r^2\overline{u}\right)}{\partial r}, \tag{39}$$

where $\delta^2 = 3\tilde{c}^2/s^2$.

Substituting equation (35) into equations (33) and (34), we get

$$\left(\frac{\partial^2}{\partial r^2} - \alpha_1\right)\overline{e} = \beta_1\frac{\partial^2\overline{\varphi}}{\partial r^2} - \delta^2\beta_1\frac{\partial^4\overline{\varphi}}{\partial r^4}, \tag{40}$$

$$\frac{\partial^2\overline{\varphi}}{\partial r^2} = \alpha_2\overline{\varphi} + \alpha_3\overline{e}, \tag{41}$$

where $\alpha_1 = s^2/(3(1 + \tau_1^\alpha s^\alpha))$, $\beta_1 = b/(1 + \tau_1^\alpha s^\alpha)$, $\alpha_2 = (s + \tau_o s^2)/(3 + \delta^2(s + \tau_o s^2))$, and $\alpha_3 = \varepsilon(s + \tau_o s^2)/(3 + \delta^2(s + \tau_o s^2))$.

Substituting equation (41) into equation (40), we obtain

$$\frac{\partial^2\overline{e}}{\partial r^2} = \alpha_4\overline{\varphi} + \alpha_5\overline{e}, \tag{42}$$

where $\alpha_4 = \beta_1\alpha_2(1 - \delta^2\alpha_2)/(1 + \delta^2\beta_1\alpha_3)$ and $\alpha_5 = (\alpha_1 + \beta_1\alpha_3(1 - \delta^2\alpha_2))/(1 + \delta^2\beta_1\alpha_3)$.

3. The Diagonalization Method

We can rewrite equations (41) and (42) in a matrix form as follows [38]:

$$\frac{\mathrm{d}}{\mathrm{d}r}\begin{bmatrix}\overline{\varphi}\\ \overline{e}\\ \overline{\varphi'}\\ \overline{e'}\end{bmatrix} = \begin{bmatrix}0 & 0 & 1 & 0\\ 0 & 0 & 0 & 1\\ \alpha_2 & \alpha_3 & 0 & 0\\ \alpha_4 & \alpha_5 & 0 & 0\end{bmatrix}\begin{bmatrix}\overline{\varphi}\\ e\\ \overline{\varphi'}\\ \overline{e'}\end{bmatrix}. \tag{43}$$

For simplicity, we write the system in (43) as a homogenous system of linear first-order differential equation as [38]

$$\frac{\mathrm{d}Z(r)}{\mathrm{d}r} = AZ(r), \tag{44}$$

where $Z(r) = \begin{bmatrix}\overline{\varphi}(r)\\ \overline{e}(r)\\ \overline{\varphi'}(r)\\ \overline{e'}(r)\end{bmatrix}$ and $A = \begin{bmatrix}0 & 0 & 1 & 0\\ 0 & 0 & 0 & 1\\ \alpha_2 & \alpha_3 & 0 & 0\\ \alpha_4 & \alpha_5 & 0 & 0\end{bmatrix}$.

Matrix A has four linearly independent eigenvectors; hence, we can construct a matrix V from the eigenvectors of matrix A such that $V^{-1}AV = W$, where W is a diagonal matrix [38].

If we make the substitution $Z = VY$ in system (44), then

$$VY' = AVY,$$
$$Y' = V^{-1}AVY = WY, \tag{45}$$

which gives

$$\begin{bmatrix}y_1'\\ y_2'\\ y_3'\\ y_4'\end{bmatrix} = \begin{bmatrix}k_1 & 0 & 0 & 0\\ 0 & k_2 & 0 & 0\\ 0 & 0 & k_3 & 0\\ 0 & 0 & 0 & k_4\end{bmatrix}\begin{bmatrix}y_1\\ y_2\\ y_3\\ y_4\end{bmatrix}, \tag{46}$$

where $\pm k_1$ and $\pm k_2$ are the eigenvalues of matrix A or the roots of the characteristic equation

$$k^4 - Lk^2 + M = 0, \tag{47}$$

where

$$L = k_1^2 + k_2^2 = \alpha_2 + \alpha_5,$$
$$M = k_1^2k_2^2 = \alpha_2\alpha_5 - \alpha_3\alpha_4,$$
$$k_2 = -k_1,$$
$$k_4 = -k_3. \tag{48}$$

Since W is a diagonal matrix, then system (46) is uncoupled, making each differential equation in the system have the form $y_i' = k_i y_i$, $i = 1, 2, 3, 4$. The solution to each of these linear equations is $y_i = c_i e^{k_i x}$, $i = 1, 2, 3, 4$. Hence, the general solution of system (46) can be written as the column vector [38]:

$$Y = \begin{bmatrix}c_1e^{k_1r}\\ c_2e^{-k_1r}\\ c_3e^{k_2r}\\ c_4e^{-k_2r}\end{bmatrix}. \tag{49}$$

Then, the final solution of system (44) is

$$Z(r) = VY(r). \tag{50}$$

Matrix V from the eigenvectors of matrix A takes the form

$$V = \begin{bmatrix} \frac{\alpha_3}{k_1\left(k_1^2 - \alpha_2\right)} & \frac{-\alpha_3}{k_1\left(k_1^2 - \alpha_2\right)} & \frac{\alpha_3}{k_2\left(k_2 - \alpha_2\right)} & \frac{-\alpha_3}{k_2\left(k_2 - \alpha_2\right)} \\ \frac{1}{k_1} & -\frac{1}{k_1} & \frac{1}{k_2} & -\frac{1}{k_2} \\ \frac{\alpha_3}{\left(k_1^2 - \alpha_2\right)} & \frac{\alpha_3}{\left(k_1^2 - \alpha_2\right)} & \frac{\alpha_3}{\left(k_2 - \alpha_2\right)} & \frac{\alpha_3}{\left(k_2 - \alpha_2\right)} \\ 1 & 1 & 1 & 1 \end{bmatrix}. \tag{51}$$

Substituting equations (49) and (51) into equation (50), we get

$$\begin{bmatrix} \overline{\varphi}(r) \\ \overline{e}(r) \\ \overline{\varphi'}(r) \\ \overline{e'}(r) \end{bmatrix} = \begin{bmatrix} \frac{\alpha_3}{k_1\left(k_1^2 - \alpha_2\right)} & \frac{-\alpha_3}{k_1\left(k_1^2 - \alpha_2\right)} & \frac{\alpha_3}{k_2\left(k_2 - \alpha_2\right)} & \frac{-\alpha_3}{k_2\left(k_2 - \alpha_2\right)} \\ \frac{1}{k_1} & -\frac{1}{k_1} & \frac{1}{k_2} & -\frac{1}{k_2} \\ \frac{\alpha_3}{\left(k_1^2 - \alpha_2\right)} & \frac{\alpha_3}{\left(k_1^2 - \alpha_2\right)} & \frac{\alpha_3}{\left(k_2 - \alpha_2\right)} & \frac{\alpha_3}{\left(k_2 - \alpha_2\right)} \\ 1 & 1 & 1 & 1 \end{bmatrix} \begin{bmatrix} c_1 e^{k_1 r} \\ c_2 e^{-k_1 r} \\ c_3 e^{k_2 r} \\ c_4 e^{-k_2 r} \end{bmatrix}. \tag{52}$$

The boundary conditions in (27) and equation (52) give that

$$\begin{aligned} c_1 &= -c_2, \\ c_3 &= -c_4. \end{aligned} \tag{53}$$

Hence, we obtain

$$\overline{\varphi}(r, s) = \alpha_3 \sum_{i=1}^{2} \frac{A_i \cosh(k_i r)}{k_i\left(k_i^2 - \alpha_2\right)}, \tag{54}$$

$$\overline{e}(r, s) = \sum_{i=1}^{2} \frac{A_i \cosh(k_i r)}{k_i}. \tag{55}$$

To get the constants A_1 and A_2, we must apply the boundary conditions at $r = a$; we consider the sphere when $r = a$ is thermally shocked as follows:

$$\varphi(a, t) = \varphi_o H(t), \tag{56}$$

where $H(t)$ is the Heaviside unit step function and φ_o is constant.

For the mechanical boundary condition, we consider the surface of the sphere when $r = a$ is connected to a rigid foundation, which can stop any displacement $(u|_{r=a} = 0)$, offering zero volumetric deformation from equation (39); hence, we have

$$e(a, t) = 0. \tag{57}$$

Applying Laplace transform on equations (56) and (57), we obtain

$$\begin{aligned} \overline{\varphi}(a, s) &= \frac{\varphi_o}{s}, \\ \overline{e}(a, s) &= 0. \end{aligned} \tag{58}$$

Applying the boundary conditions in equations (54) and (55), we get the following system:

$$\sum_{i=1}^{2} \frac{A_i \cosh(k_i a)}{k_i\left(k_i^2 - \alpha_2\right)} = \frac{\varphi_0}{s\alpha_3}, \tag{59}$$

$$\sum_{i=1}^{2} \frac{A_i \cosh(k_i a)}{k_i} = 0. \tag{60}$$

By solving system (59) and (60) by using the relations between the roots (48), we get

$$A_1 = \frac{\varphi_0 \alpha_4 k_1}{s\left(k_1^2 - k_2^2\right)\cosh(k_1 a)},$$
$$A_2 = -\frac{\varphi_0 \alpha_4 k_2}{s\left(k_1^2 - k_2^2\right)\cosh(k_2 a)}. \tag{61}$$

Hence, we have

$$\overline{\varphi}(r,s) = \frac{\varphi_0 \alpha_3 \alpha_4}{s\left(k_1^2 - k_2^2\right)}\left[\frac{\cosh(k_1 r)}{\left(k_1^2 - \alpha_2\right)\cosh(k_1 a)} - \frac{\cosh(k_2 r)}{\left(k_2^2 - \alpha_2\right)\cosh(k_2 a)}\right], \tag{62}$$

$$\overline{e}(r,s) = \frac{\varphi_0 \alpha_4}{s\left(k_2^2 - k_1^2\right)}\left[\frac{\cosh(k_1 r)}{\cosh(k_1 a)} - \frac{\cosh(k_2 r)}{\cosh(k_2 a)}\right]. \tag{63}$$

To obtain the displacement function, we will use equations (39) and (63) as

$$\overline{u}(r,s) = \frac{1}{r^2}\int r^2 \overline{e}(r,s)\partial r. \tag{64}$$

The singularity in (64) can be removed by using L'Hopital's rule twice in a row as follows [36]:

$$\overline{u}(r,s) = \lim_{r \longrightarrow 0} \frac{\int\left(r^2 \overline{e}(r,s)\right)\partial r}{r^2} = \lim_{r \longrightarrow 0} \frac{r^2 \overline{e}(r,s)}{2r} = \frac{r\overline{e}(r,s)}{2}. \tag{65}$$

Hence, we have

$$\overline{u}(r,s) = \frac{\varphi_0 \alpha_4 r}{2s\left(k_2^2 - k_1^2\right)}\left[\frac{\cosh(k_1 r)}{\cosh(k_1 a)} - \frac{\cosh(k_2 r)}{\cosh(k_2 a)}\right]. \tag{66}$$

We use the average of the three principal stress components for equations (36)–(38) to achieve a straightforward way of distribution to be as follows:

$$\overline{\sigma}(r,s) = \frac{\overline{\sigma_{rr}} + \overline{\sigma_{\psi\psi}} + \overline{\sigma_{\phi\phi}}}{3} = \left(\beta^2 - \frac{4}{3}\right)(1-D)\overline{e}(r,s) - \varepsilon_1 (1-D)\overline{\theta}(r,s). \tag{67}$$

The techniques of Riemann-sum approximation are used to obtain numerical solutions of studied functions in the time domain. In this method, any function can be transformed into the Laplace by using the following formula [39]:

$$f(t) = \frac{e^{\kappa t}}{t}\left[\frac{1}{2}\overline{f}(\kappa) + \mathrm{Re}\sum_{n=1}^{N}(-1)^n \overline{f}\left(\kappa + \frac{in\pi}{t}\right)\right], \tag{68}$$

where "i" is the well-known unit of imaginary number and "Re" gives the real part. Many computational studies have shown that value κ meets the relationship for convergence with faster procedures. $\kappa t \approx 4.7$ [39].

After calculating the Laplace transformations, the stress-strain energy can be obtained in the following formula [40]:

$$\omega(r,t) = \frac{1}{2}\sigma_{ij}(r,t)e_{ij}(r,t). \tag{69}$$

For the current model, the stress-strain energy is in the form

$$\omega(r,t) = \frac{1}{2}\left(\sigma_{rr}e_{rr} + \sigma_{\psi\psi}e_{\psi\psi} + \sigma_{\phi\phi}e_{\phi\phi}\right). \tag{70}$$

After eliminating the term with a small value, we get

$$\omega(r,t) \approx \frac{1}{2}\left[\left(1 + \tau_1^{\alpha} D_t^{\alpha}\right)\beta^2 e^2(r,t) - \varepsilon_1 e(r,t)\theta(r,t)\right]. \tag{71}$$

4. Numerical Results and Discussion

For numerical analysis, copper is the thermoelastic substance for which the various physical constants' values are taken as follows [24]:

$$\begin{aligned} K &= 386\,\mathrm{kg\,m\,k^{-1}s^{-3}},\\ \alpha_T &= 1.78(10)^{-5}\,\mathrm{k^{-1}},\\ \rho &= 8954\,\mathrm{kg\,m^{-3}},\\ T_o &= 293\,\mathrm{k},\\ C_E &= 383.1\,\mathrm{m^2\,k^{-1}\,s^{-2}},\\ \mu &= 3.86(10)^{10}\,\mathrm{kg\,m^{-1}\,s^{-2}},\\ \lambda &= 7.76(10)^{10}\mathrm{kg\,m^{-1}\,s^{-2}}. \end{aligned} \tag{72}$$

Thus, we get the nondimensional values of the problem as

$$\begin{aligned} b &= 0.01047,\\ \varepsilon_1 &= 0.0419,\\ \varepsilon &= 1.6086\\ \beta^2 &= 4,\\ \varphi_0 &= 1.0,\\ \tau_o &= 0.02,\\ \tau_o &= 0.01. \end{aligned} \tag{73}$$

For a large range of the dimensionless radial distance, r $(0 \le r \le 8.0)$, the numerical results from conductive and dynamic temperature increments, pressure, changes, average stress, and stress-power distributions were shown at the instant value of dimensionless time $t = 1.0$.

Figures 2–7 were obtained for various values of the two-temperature parameter $\widetilde{c} = (0.0, 0.5)$, which gives $\delta^2 = 3\widetilde{c}^2/s^2 = (0.0, 3(0.5)^2, 3(0.5/s)^2)$, where the value $\delta = 0.0$ represents the L-S one-temperature model; it has been figured in solid curves. The value $\widetilde{c} = 0.5$ represents two cases; the first case is $\delta^2 = 3(0.5)^2$, which represents the classical two-temperature model and has been figured with dash

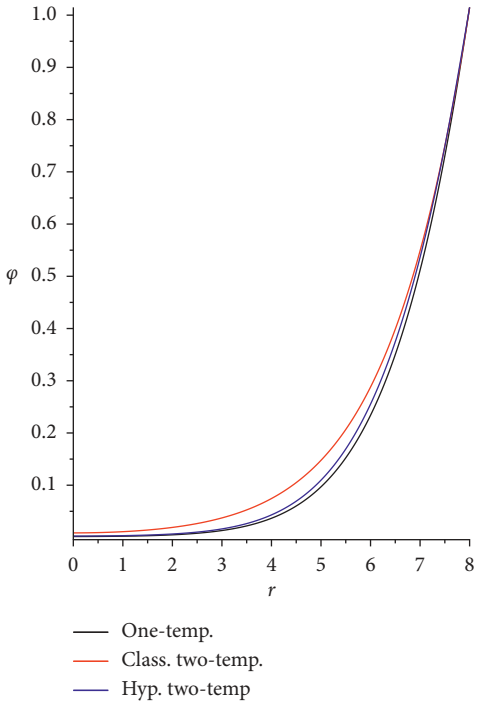

Figure 2: The conductive temperature increment distribution for different models.

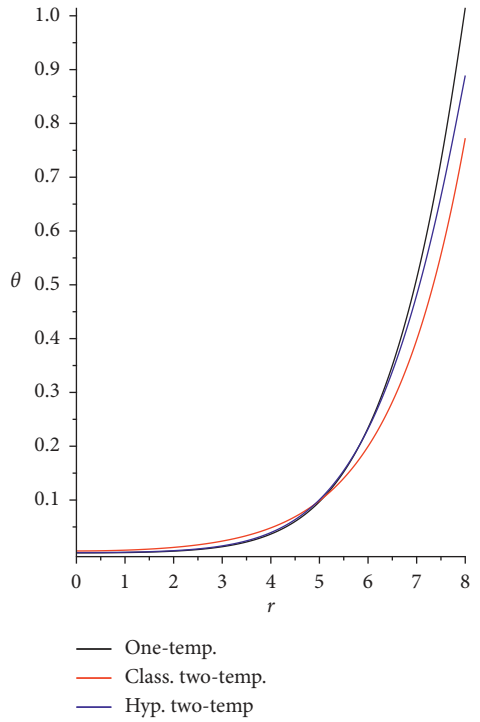

Figure 3: The dynamical temperature increment distribution for different models.

curves, while the second case is $\delta^2 = 3(0.5/s)^2$, which represents the hyperbolic two-temperature model and has been figured in dot curves. The numerical results of those figures have been calculated when the fractional order parameter $\alpha = 0.5$.

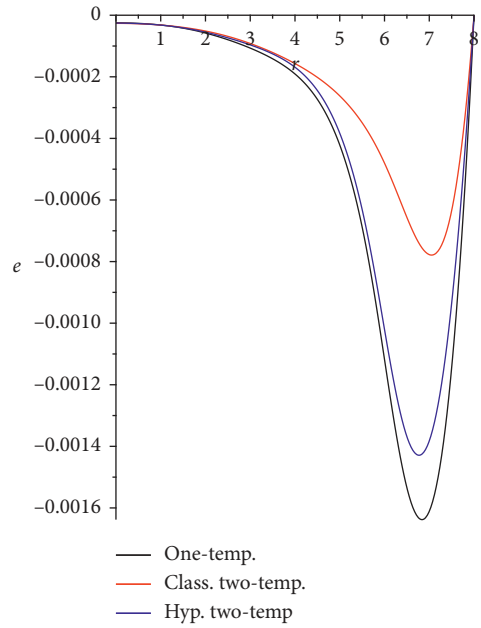

Figure 4: The volumetric deformation distribution for different models.

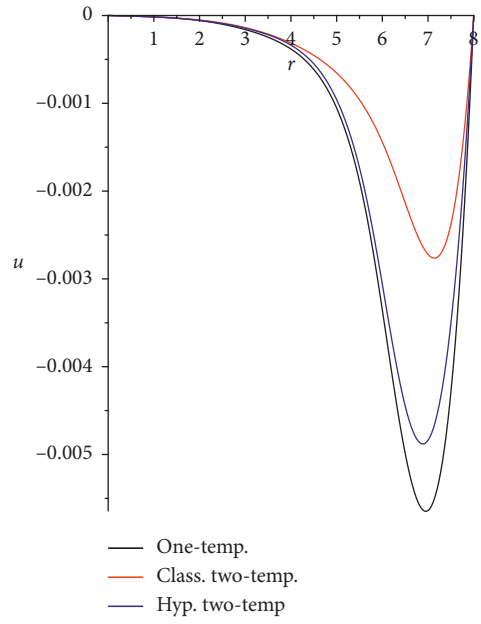

Figure 5: The displacement distribution for different models.

Figure 2 shows the conductive temperature increment distributions, and it is seen that all the curves start from the position $r = 8.0$ with the value $\varphi(r = 8.0) = 1.0$, which is the value of the thermal shock on the bounding surface of the sphere. All the curves have the same behavior but with different values. The two-temperature parameter has a significant effect on conductive temperature distribution. At the endpoint of the sphere's radius, the one-temperature and hyperbolic two-temperature model curves fall to zero values. It means that the conductive thermal wave has propagated with a finite speed in the context of one-temperature and

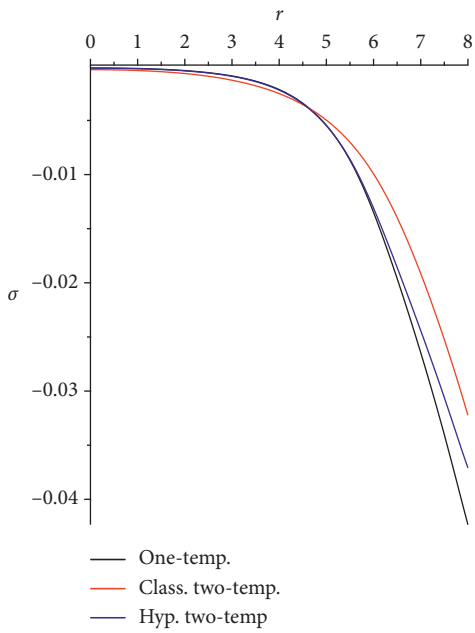

Figure 6: The average stress distribution for different models.

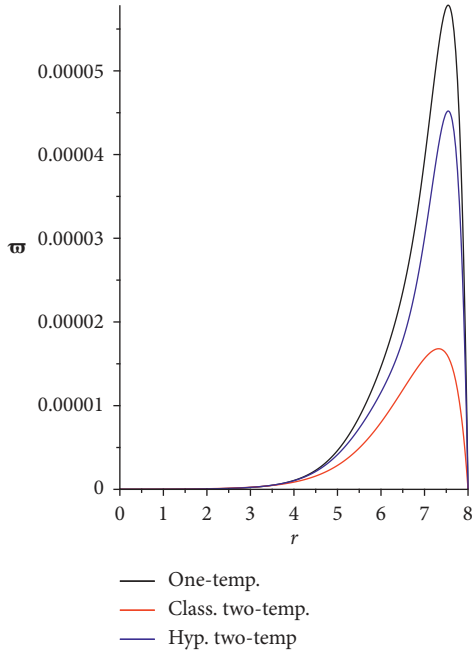

Figure 7: The stress-strain energy distribution for different models.

hyperbolic two-temperature models, while the classical two-temperature model does not.

Figure 3 shows the dynamical temperature increment distributions, where it is noted that all the curves start from the position $r = 8.0$ with different values $\theta|_{\text{one-temp.}} = 1.0$, which is the value of the thermal shock on the bounding surface of the sphere $\theta|_{\text{Class. two-temp.}} = 0.98$ and $\theta|_{\text{hyp. two-temp.}} = 0.75$. All the curves have the same behavior with various values. The two-temperature parameter has a significant effect on the dynamical temperature distribution. At the endpoint of the sphere's radius, the one-temperature and hyperbolic two-temperature model curves fall to zero values. It means that the dynamical thermal wave has propagated with a finite speed in the context of one-temperature and hyperbolic two-temperature models, while the classical two-temperature model does not.

The volumetric distribution of the strain is illustrated in Figure 4, and three curves begin at $r = 8.0$, a position with zero value $e(r = 8.0) = 0.0$, which agrees with the boundary condition on the sphere's bounding surface. All the curves have the same attitude with different values. The one-temperature and hyperbolic two-temperature models' curves have a sharp point in the same position with different values. In contrast, the classical two-temperature model has a peak point in different situations. The absolute values of the maximum volumetric deformation take the following order:

$$\begin{aligned}\left|e_{\max}(\text{One}-\text{temp.})\right| &> \left|e_{\max}(\text{Hyp. two}-\text{temp.})\right| \\ &> \left|e_{\max}(\text{Class. two}-\text{temp.})\right|.\end{aligned} \tag{74}$$

Figure 5 shows the displacement distributions, and it is seen that the three curves start from the position $r = 8.0$ with zero value $u(r = 8.0) = 0.0$. All the curves have the same attitude with various values. The one-temperature and hyperbolic two-temperature models' curves have sharp points in the same position with different values. In contrast, the classical two-temperature model has a peak point in different situations. The absolute values of the maximum displacement take the following order:

$$\begin{aligned}\left|u_{\max}(\text{One}-\text{temp.})\right| &> \left|u_{\max}(\text{Hyp. two}-\text{temp.})\right| \\ &> \left|u_{\max}(\text{Class. two}-\text{temp.})\right|.\end{aligned} \tag{75}$$

Figure 6 represents the average stress distributions, and we can see that the three curves start from the position $r = 8.0$ with different values. The one- and two-temperature curves have the same behavior with different values, and each has a sharp point. The curve, by comparison, is distinct and smooth in the classical two-temperature model.

Figure 7 shows the stress-strain energy distribution, and it is noted that the three curves start from the position $r = 8.0$ with zero values. The three curves have the same behavior with different values, and each one has a peak point. The maximum values of the stress-strain energy take the following order:

$$\begin{aligned}\left|\varpi_{\max}(\text{One}-\text{temp.})\right| &> \left|\varpi_{\max}(\text{Hyp. two}-\text{temp.})\right| \\ &> \left|\varpi_{\max}(\text{Class. two}-\text{temp.})\right|.\end{aligned} \tag{76}$$

Figures 8–13 have been done for different values of the fractional-order parameter $\alpha = (0.0\,(\tau_1 = 0), 0.2, 0.6, 1.0)$ in the context of the hyperbolic two-temperature model to discuss its effects on the state of the studied functions. The case $\alpha = \tau_1 = 0.0$ represents the normal stress-strain relations as the usual Hooke's law of the elastic body. In contrast, the cases $\alpha = (0.2, 0.6)$ define the new cases between the normal elasticity and the viscoelasticity and $\alpha = 1.0$ represents the viscoelasticity.

Figures 8 and 9 show that the fractional-order parameter has limited impacts on the dynamical and conductive

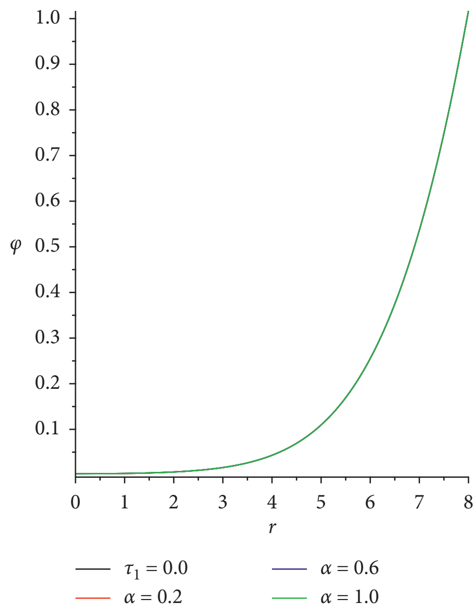

Figure 8: The conductive temperature increment distribution with various values of the fractional-order parameter.

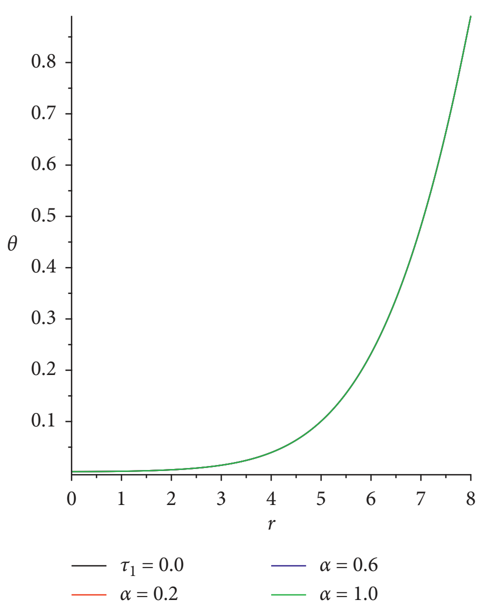

Figure 9: The dynamical temperature increment distribution with various values of the fractional-order parameter.

temperature increment. This result was expected because the fractional-order parameter's effect exists firmly in the stress-strain relation, which significantly influences the mechanical waves more than the thermal waves.

Figure 10 represents that the effect of the fractional-order parameter is significant on the volumetric strain distributions. All the curves start from the position $r = 8.0$ with zero value, and every curve contains a peak except for the curve, which has no fraction $\tau_1 = 0.0$, and it has a sharp point. The maximum values of the absolute value of the volumetric deformation take the following order:

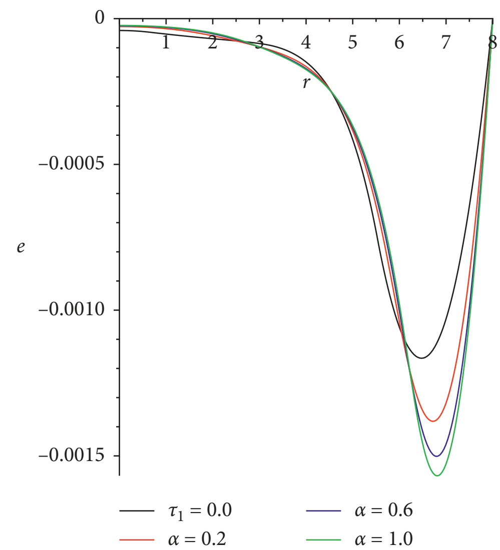

Figure 10: The volumetric deformation distribution with various values of the fractional-order parameter.

$$\left|e_{\max}(\alpha = 1.0)\right| > \left|e_{\max}(\alpha = 0.6)\right| > \left|e_{\max}(\alpha = 0.2)\right| > \left|e_{\max}(\alpha = \tau_1 = 0.0)\right|. \quad (77)$$

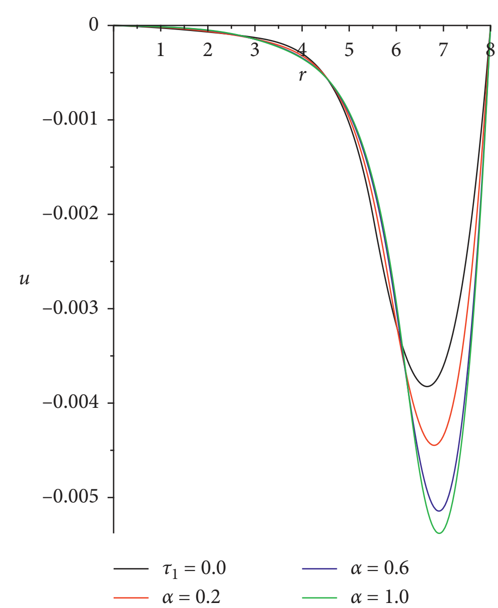

Figure 11: The displacement distribution with various values of the fractional-order parameter.

Figure 11 indicates a significant influence on displacement distributions of the fractional-order parameter. The four curves begin at the location $r = 8.0$, and each curve contains a peak except the curve, which does not have a fraction $\tau_1 = 0.0$, where it has a sharp point. The maximum values of the absolute value of the displacement take the following order:

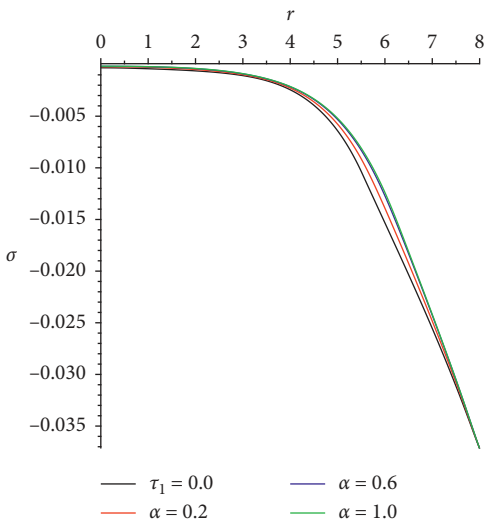

FIGURE 12: The average stress distribution with various values of the fractional-order parameter.

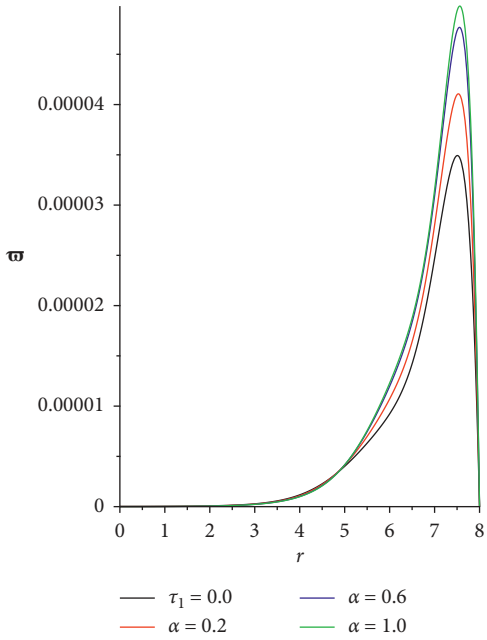

FIGURE 13: The stress-strain energy distribution with various values of the fractional-order parameter.

$$\left|u_{\max}(\alpha = 1.0)\right| > \left|u_{\max}(\alpha = 0.6)\right| > \left|u_{\max}(\alpha = 0.2)\right| > \left|u_{\max}(\alpha = \tau_1 = 0.0)\right|. \tag{78}$$

Figure 12 represents that the fractional-order parameter has significant impacts on stress distributions. All the curves start from the position $r = 8.0$ with the same value, and each curve is smooth except the curve of the case, which has no fraction $\tau_1 = 0.0$, and it has a sharp point.

Figure 13 represents that the fractional-order parameter has significant effects on stress-strain energy distributions. The four curves start from the position $r = 8.0$ with zero values, and each curve has a peak point. The values of the maximum stress-strain energy take the following order:

$$\left|\varpi_{\max}(\alpha = 1.0)\right| > \left|\varpi_{\max}(\alpha = 0.6)\right| > \left|\varpi_{\max}(\alpha = 0.2)\right| > \left|\varpi_{\max}(\alpha = \tau_1 = 0.0)\right|. \tag{79}$$

For the validation of the results, we can notice that the current results that are based on traditional integer derivative agree with the results in the past publications [25, 28, 29, 32, 41–43].

5. Conclusions

The numerical results conclude that the one-temperature model and the hyperbolic two-temperature theory of thermoelasticity generate thermomechanical waves that can propagate with limited speeds. Therefore, the hyperbolic two-temperature thermoelasticity model is a successful model to describe thermoelastic materials' thermodynamical behavior. Moreover, the two-temperature parameter has significant impacts on the states of all the studied functions. The fractional-order strain parameter has weak effects on the thermal waves, while its effects on the mechanical waves are significant.

Abbreviations

C_E: Specific heat at constant strain
c_o: $= \sqrt{(\lambda + 2\mu)/\rho}$ longitudinal wave speed
e_{ij}: The strain components
K: Thermal conductivity
T_D, T_C: Dynamical and conductive temperature, respectively
T_o: Reference temperature
t: Time
u_{ij}: The displacement components
α_T: Coefficient of linear thermal expansion
β: $= ((\lambda + 2\mu)/\mu)^{1/2}$
γ: $= (3\lambda + 2\mu)\alpha_T$
ε: $= \gamma/\rho C_E$, the mechanical coupling constant (dimensionless)
ε_1: $= \gamma T_o/\mu$, the thermoelastic coupling constant (dimensionless)
η: $= \rho C_E/K$, the thermal viscosity
λ, μ: Lamé constants
ρ: Density
σ_{ij}: The stress tensor of components
τ_0: Thermal relaxation time.

Data Availability

No data were used to support this study.

Conflicts of Interest

The authors declare that there are no conflicts of interest.

References

[1] P. J. Chen and M. E. Gurtin, "On a theory of heat conduction involving two temperatures," *Zeitschrift für angewandte Mathematik und Physik ZAMP*, vol. 19, no. 4, pp. 614–627, 1968.

[2] W. Warren and P. Chen, "Wave propagation in the two temperature theory of thermoelasticity," *Acta Mechanica*, vol. 16, no. 1-2, pp. 21–33, 1973.

[3] H. M. Youssef, "Theory of two-temperature-generalized thermoelasticity," *IMA Journal of Applied Mathematics*, vol. 71, no. 3, pp. 383–390, 2006.

[4] I. A. Abbas and H. M. Youssef, "Two-temperature generalized thermoelasticity under ramp-type heating by finite element method," *Meccanica*, vol. 48, no. 2, pp. 331–339, 2013.

[5] H. Youssef, "Two-temperature generalized thermoelastic infinite medium with cylindrical cavity subjected to different types of thermal loading," *WSEAS Transactions on Heat and Mass Transfer*, vol. 1, no. 10, p. 769, 2006.

[6] H. Youssef, "A two-temperature generalized thermoelastic medium subjected to a moving heat source and ramp-type heating: a state-space approach," *Journal of Mechanics of Materials and Structures*, vol. 4, no. 9, pp. 1637–1649, 2010.

[7] H. M. Youssef, "Two-temperature generalized thermoelastic infinite medium with cylindrical cavity subjected to non-gaussian laser beam," *Journal of Thermoelasticity*, vol. 1, no. 2, pp. 13–18, 2013.

[8] H. M. Youssef, "Two-dimensional problem of a two-temperature generalized thermoelastic half-space subjected to ramp-type heating," *Computational Mathematics and Modeling*, vol. 19, no. 2, pp. 201–216, 2008.

[9] H. M. Youssef, "Two-temperature generalized thermoelastic infinite medium with cylindrical cavity subjected to moving heat source," *Archive of Applied Mechanics*, vol. 80, no. 11, pp. 1213–1224, 2010.

[10] H. M. Youssef and A. A. El-Bary, "Characterization of the photothermal interaction of a semiconducting solid sphere due to the mechanical damage and rotation under Green-Naghdi theories," *Mechanics of Advanced Materials and Structures*, pp. 1–16, 2020.

[11] A. M. Zenkour, "Refined two-temperature multi-phase-lags theory for thermomechanical response of microbeams using the modified couple stress analysis," *Acta Mechanica*, vol. 229, no. 9, pp. 3671–3692, 2018.

[12] A. Abouelregal and A. Zenkour, "Two-temperature thermoelastic surface waves in micropolar thermoelastic media via dual-phase-lag model," *Advances in Aircraft and Spacecraft Science*, vol. 4, no. 6, p. 711, 2017.

[13] A. E. Abouelregal and A. M. Zenkour, "A generalized thermoelastic medium subjected to pulsed laser heating via a two-temperature model," *Journal of Theoretical and Applied Mechanics*, vol. 57, no. 3, pp. 631–639, 2019.

[14] H. M. Youssef and A. A. El-Bary, "Theory of hyperbolic two-temperature generalized thermoelasticity," *Materials Physics and Mechanics*, vol. 40, pp. 158–171, 2018.

[15] W. M. Ahmad and R. El-Khazali, "Fractional-order dynamical models of love," *Chaos, Solitons & Fractals*, vol. 33, no. 4, pp. 1367–1375, 2007.

[16] A. Sur and S. Mondal, "Effect of non-locality in the vibration of a micro-scale beam under two-temperature memory responses," *Waves in Random and Complex Media*, pp. 1–28, 2020.

[17] C. Zhao, D. Xue, and Y. Chen, "A fractional order PID tuning algorithm for a class of fractional order plants," in *Proceedings of the 2005 IEEE International Conference Mechatronics and Automation*, pp. 216–221, IEEE, Niagara Falls, Ontario, Canada, August 2005.

[18] A. Sur, "Memory response on wave propagation in a micropolar magneto-thermo-viscoelastic half-space," *Waves in Random and Complex Media, Waves in Random and Complex Media*, pp. 1–29, 2020.

[19] R. L. Magin and T. J. Royston, "Fractional-order elastic models of cartilage: a multi-scale approach," *Communications in Nonlinear Science and Numerical Simulation*, vol. 15, no. 3, pp. 657–664, 2010.

[20] H. M. Youssef, "Theory of generalized thermoelasticity with fractional order strain," *Journal of Vibration and Control*, vol. 22, no. 18, Article ID 1077546314566837, 2015.

[21] H. Youssef, "State-space approach on generalized thermoelasticity for an infinite material with a spherical cavity and variable thermal conductivity subjected to ramp-type heating," *Canadian Applied Mathematics Quarterly*, vol. 13, p. 4, 2005.

[22] H. M. Youssef, "Dependence of modulus of elasticity and thermal conductivity on reference temperature in generalized thermoelasticity for an infinite material with a spherical cavity," *Applied Mathematics and Mechanics*, vol. 26, no. 4, pp. 470–475, 2005.

[23] H. M. Youssef and A. H. Al-Harby, "State-space approach of two-temperature generalized thermoelasticity of infinite body with a spherical cavity subjected to different types of thermal loading," *Archive of Applied Mechanics*, vol. 77, no. 9, pp. 675–687, 2007.

[24] H. M. Youssef, "Generalized thermoelastic infinite medium with spherical cavity subjected to moving heat source," *Computational Mathematics and Modeling*, vol. 21, no. 2, pp. 212–225, 2010.

[25] S. Mukhopadhyay and R. Kumar, "A study of generalized thermoelastic interactions in an unbounded medium with a spherical cavity," *Computers & Mathematics with Applications*, vol. 56, no. 9, pp. 2329–2339, 2008.

[26] M. A. K. Molla, N. Mondal, and S. H. Mallik, "Effects of fractional and two-temperature parameters on stress distributions for an unbounded generalized thermoelastic medium with spherical cavity," *Arab Journal of Basic and Applied Sciences*, vol. 26, no. 1, pp. 302–310, 2019.

[27] S. Mondal and A. Sur, "Photo-thermo-elastic wave propagation in an orthotropic semiconductor with a spherical cavity and memory responses," *Waves in Random and Complex Media*, pp. 1–24, 2020.

[28] E. A. Al-Lehaibi, "Mathematical model of generalized thermoelastic infinite medium with a spherical cavity and fractional order strain," *Journal of Nonlinear Sciences & Applications (JNSA)*, vol. 12, no. 1, 2019.

[29] W. Peng, Y. Ma, C. Li, and T. He, "Dynamic analysis to the fractional order thermoelastic diffusion problem of an infinite body with a spherical cavity and variable material properties," *Journal of Thermal Stresses*, vol. 43, no. 1, pp. 38–54, 2020.

[30] M. I. A. Othman, E. M. Abd-Elaziz, and M. I. M. Hilal, "State-space approach to a 2-D generalized thermoelastic medium under the effect of inclined load and gravity using a dual-phase-lag model," *Mechanics Based Design of Structures and Machines*, pp. 1–17, 2020.

[31] H. H. Sherief and E. M. Hussein, "The effect of fractional thermoelasticity on two-dimensional problems in spherical regions under axisymmetric distributions," *Journal of Thermal Stresses*, vol. 43, no. 4, pp. 440–455, 2020.

[32] S. Biswas, "Thermoelastic interaction in unbounded transversely isotropic medium containing spherical cavity with energy dissipation," *Indian Journal of Physics*, pp. 1–12, 2020.
[33] D. K. Sharma, M. Bachher, and N. Sarkar, "Effect of phase-lags on the transient waves in an axisymmetric functionally graded viscothermoelastic spherical cavity in radial direction," *International Journal of Dynamics and Control*, pp. 1–14, 2020.
[34] P. Lata and H. Kaur, "Effect of two temperature on isotropic modified couple stress thermoelastic medium with and without energy dissipation," *Geomechanics and Engineering*, vol. 21, no. 5, pp. 461–469, 2020.
[35] E. M. Hussein, "Two dimensional spherical regions problem in the context of the theory of generalized thermoelastic diffusion," *Journal of Thermal Stresses*, vol. 43, no. 9, pp. 1–15, 2020.
[36] J. Thibault, S. Bergeron, and H. Bonin, "On finite-difference solutions of the heat equation in spherical coordinates," *Numerical Heat Transfer, Part B: Fundamentals*, vol. 12, no. 4, pp. 457–474, 1987.
[37] Y. Povstenko, *Fractional Thermoelasticity*, Springer, Berlin, Germany, 2015.
[38] D. Zill, W. S. Wright, and M. R. Cullen, *Advanced Engineering Mathematics*, S. Chand Publishing, Mathura Road, New Delhi, 2011.
[39] D. Y. Tzou, "A unified field approach for heat conduction from macro- to micro-scales," *Journal of Heat Transfer*, vol. 117, no. 1, pp. 8–16, 1995.
[40] Z. Chen and A. Akbarzadeh, *Advanced Thermal Stress Analysis of Smart Materials and Structures*, Springer, Berlin, Germany, 2020.
[41] I. A. Abbas, "Eigenvalue approach for an unbounded medium with a spherical cavity based upon two-temperature generalized thermoelastic theory," *Journal of Mechanical Science and Technology*, vol. 28, no. 10, pp. 4193–4198, 2014.
[42] N. A. Alghamdi and H. M. Youssef, "On the application of the adomian's decomposition method to a generalized thermoelastic infinite medium with a spherical cavity in the framework three different models," *Fluid Dynamics & Materials Processing*, vol. 15, no. 5, pp. 597–611, 2019.
[43] H. M. Youssef, "Generalized thermoelasticity of an infinite body with a cylindrical cavity and variable material properties," *Journal of Thermal Stresses*, vol. 28, no. 5, pp. 521–532, 2005.